PROCEEDINGS OF ECOS 2023 - THE 36TH INTERNATIONAL CONFERENCE ON
EFFICIENCY, **C**OST, **O**PTIMIZATION, **S**IMULATION AND ENVIRONMENTAL IMPACT OF ENERGY SYSTEMS
25-30 JUNE 2023, LAS PALMAS DE GRAN CANARIA, SPAIN

Thermodynamic and economic analysis of a Carnot battery with a two-zone water tank as thermal energy storage

Josefine Koksharov[a], Jonas Klingelhöfer[a], Frank Dammel[a], Peter Stephan[a]

[a] *Institute for Technical Thermodynamics, Technical University of Darmstadt, Darmstadt, Germany, koksharov@ttd.tu-darmstadt.de, CA*

Abstract:

In the process of energy transition, the share of renewable energy sources is increasing. This leads to strong fluctuations in power generation. To balance supply and demand, energy storage is required. Carnot batteries could be a promising storage technology to solve this problem. These batteries convert electrical energy into thermal energy through an electrical resistance heater or a heat pump and stores this energy for a period of time. Later, the thermal energy is converted back into electrical energy through a heat engine.

A Carnot battery with a two-zone tank and water as a storage medium was investigated. This type of storage allows storage temperatures above 100 °C under atmospheric conditions. The system studied here applies a storage temperature of 115 °C. Charging is realized with a CO_2 heat pump, while discharging uses a heat engine with an organic fluid. This Carnot battery was implemented and simulated in EBSILON®*Professional*. The supplied electrical power was 18 MW and the maximum outlet temperature was 150 °C. Derived from the day-ahead market [1], a charging and discharging time of 4 h was applied. To identify the most promising concept for practical applications, the round trip efficiency, levelized cost of electricity (LCOE), and technology readiness level (TRL) of the different Carnot battery configurations were compared. In addition, a simplified sensitivity analysis was performed to assess the influence of the uncertainties of the economic parameters on the LCOE. Furthermore, the change in the LCOE with a variation in the charging and discharging duration was investigated.

The advantage of a CO_2 heat pump is that applications with high input power have already been implemented, which leads to an estimated TRL of at least 6. By contrast, heat pumps for temperatures above 100 °C utilizing screw or piston compressors are only available for lower power applications.

Keywords:

Carnot Battery, CO_2 Heat Pump, Organic Rankine Cycle, Water Storage Tank.

1. Introduction

Electricity generation from renewable energy is subject to fluctuations due to weather conditions. To ensure a secure power supply with an increasing share of renewable energy, energy storage systems are needed to temporarily store electrical energy, and thus compensate for fluctuations. Pumped thermal electricity storages, known as a Carnot battery (CB), is a promising technology in this respect. A CB is a system that converts electrical energy into thermal energy through an electrical resistance heater or a heat pump and stores this energy for a period of time. Later, the thermal energy is converted back into electrical energy through a heat engine. CBs have been studied in different configurations involving supercritical, transcritical, and subcritical processes [2]. Comprehensive overviews of CBs can be found in [2, 3]. For storing thermal energy, sensible, latent, or thermo-chemical energy storage systems are available. A sensible energy storage system consists of a single storage tank with a thermocline (stratified storage) or two tanks, where the storage medium is pumped from one tank into the other.

An overview of the research literature is given below. This study focuses on configurations in which CO_2 transcritical processes are used. Several authors dealing with CBs have considered transcritical processes predominantly using CO_2 [4–11] as a working fluid. Energy storage on the hot side is often realized in tanks with hot water [4, 7, 8, 10]. This allows a temperature glide between the storage medium (water) and the working fluid. On the cold side, either an ice storage tank [4, 7] or the environment [10, 11] are considered as storage units.

Mercangöz et al. [9] described a transcritical charging and discharging process using CO_2 as a working fluid. The concept included two storage units, one of which stored thermal energy at higher temperatures in water

https://doi.org/10.52202/069564-0192

tanks at a maximum temperature of 123 °C and the other stored energy in an ice storage tank at a temperature of -5 °C. Because of the irreversibilities that occur in the process, the ice storage is supplemented by an additional circuit during the charging process to dissipate losses to the environment. With a nominal turbine power of 1 MW ($\eta_{turbine}$ = 86 %, $\eta_{compressor}$ = 81.5 %, $\eta_{expander}$ = 80 %, and η_{pump} = 80 %) for a pilot project and a nominal turbine power of 50 MW ($\eta_{turbine}$ = 91 %, $\eta_{compressor}$ = 89 %, $\eta_{expander}$ = 88 %, and η_{pump} = 86 %) for a commercial plant, round trip efficiencies of 51 % and 65 %, respectively, were achieved.

Morandin [4,5], starting from the base case, optimized the transcritical CO_2 charging and discharging process. The base case included, on the hot side, a sensible energy storage system using water as a storage medium, with several tanks storing energy at different temperatures, and, on the cold side, an ice storage system consisting of two tanks. The ice storage tank contained a salt mixture to lower the freezing point to -21.2 °C. An air fan was also integrated into the charging and discharging process to release the resulting irreversibilities to the environment in the form of heat. By optimizing the base case with eight water tanks and a maximum discharge temperature of 177 °C, a round trip efficiency of 60 % was achieved. By adding an internal heat exchanger in the charging and discharging process to the base case configuration, the round trip efficiency was increased to 62 %. The expansion of the working fluid occurs in the two phase/wet steam area, which is associated with technological problems. To prevent these problems, a throttle can be used instead of the expander, which in turn leads to a drop in round trip efficiency.

Another study on CB was presented by Kim et al. [8], based on Morandin and Mercangöz [4,9]. Nevertheless, in the study by Kim et al. [8] the concept involved isothermal compression/expansion using a liquid expander and a water injection to cool the working fluid during the charging process and to heat it during the discharging process, respectively. At a maximum pressure of 160 bar and a maximum charging temperature of 150 °C, and under high isentropic efficiencies ($\eta_{compressor,charging}$ = 90 %, $\eta_{expander,charging}$ = 85 %, $\eta_{compressor,discharging}$ = 0.85 %, $\eta_{expander,discharging}$ = 90%) an overall efficiency of 74.5 % was obtained.

Steinmann et al. [7] studied a CB that consisted of transcritical CO_2 cycles and two storage units at different temperatures. The first storage unit was a pressurized water storage tank with a temperature up to 160 °C. The other one was an ice storage unit with a temperature of 0 °C. With an isentropic compressor and turbine efficiency between 80 % and 90, % the round trip efficiency was about 45 %.

Baik et al. [10] investigated CBs with a transcritical CO_2 process involving two-tank liquid systems, each on the hot and cold side. The tanks on the cold side used the environment with a temperature of 20 °C as a heat source and heat sink, respectively. These storage tanks were operated with water. Compared to the concepts in [4,5,7], a throttle was integrated into the charging process instead of an expander. The maximum storage temperature was 120 °C and isentropic efficiencies of 85 % were assumed for the: compressor, turbine, and pump. The round trip efficiency was studied as a function of the lower storage temperature of the two-tank system on the hot side, which varied between 25 and 70 °C. Under these conditions, round trip efficiencies ranged from 14.7 % to 29.1 %, with the maximum reached at the lower storage temperature of 40 °C on the hot side.

Koen et al. [11] analyzed the transcritical process by testing different working fluids, such as CO_2, R1234yf, R1234ze(e), R1234ze(z), R152A, R161, R13I1, and ammonia, and different storage media such as water,Therminol D12, and Therminol 66. The concept included a compressor and an expander for both charging and discharging processes. A storage unit was implemented on the hot side, designed as a two-tank system. A low-temperature storage tank was dispensed, with and thus, a heat exchanger used the environment as the second storage unit. Under optimal operation conditions with polytropic component efficiencies of 90 %, round trip efficiencies between 50.5 % and 57.6 % were obtained. The best result was achieved using the working fluid R13I1 at a maximal storage temperature of 206 °C.

The described concepts generally use the round trip efficiency to evaluate their configurations. In this study, besides the round trip efficiency, the levelized cost of electricity (LCOE) and the technology readiness level (TRL) were determined to answer the following questions:

With which CBs could a system be realized in a timely manner?

Which efficiencies are achieved and what are the resulting LCOEs of the investigated CBs?

How does reducing the pinch point of the heat exchangers affect the round trip efficiency, purchased equipment cost, and LCOE?

The study focuses on various CB concepts based on the transcritical charging process with CO_2 as a working fluid. Using CO_2, an appropriate compressor at an outlet temperature greater than 100 °C, allows the implementation of a heat pump at a larger scale [12,13]. So far, it is only possible to implement heat pumps in the kW range with positive displacement machines, using a high compressor discharge temperature [14]. A two-zone storage tank is used as a thermal energy storage (TES). This type of storage consists of an upper and a lower chamber, which are separated from each other by a partition wall. These chambers are filled with water

https://doi.org/10.52202/069564-0192

at different temperatures and are connected by pipes. The water in the upper chamber exerts pressure on the lower chamber. This allows the storage of water in the lower chamber in a pressureless state at temperatures $> 100\,°C$. Compared to pressure-loaded tanks with water, the two-zone storage tank is a safer and cheaper option [15]. In combination with the two-zone storage tank, the working fluid (CO_2) is suitable for the transcritical charging process. This mode of operation has the advantage that the CO_2 approximates the course of the temperature glide of the storage medium (water) in the two-zone storage tank. One way to discharge the TES is to use a heat engine, which is also operated with the same working fluid (CO_2) in transcritical mode. Alternatively, subcritical processes with different organic working fluids can be considered as these subcritical processes are already used in practice, (e.g., in geothermal plants) [16].

2. Design and Simulation of the Carnot Battery

The CB consists of a transcritical charging process and a sensible thermal energy storage (TES). The discharge of the TES is either transcritical or subcritical. The schemes of the charging and discharging subprocesses are shown in Fig. 1 a) and b), respectively. The subprocesses are described below.

Charging Process

Excess electrical energy is used to compress the working fluid to a supercritical pressure (HP1-HP2). After transferring the heat to the TES (HP2-HP3), the working fluid is further cooled in the regenerative heat exchanger (HP3-HP4) until the liquid state is reached. Then, the working fluid is first expanded in a liquid expander to a nearly saturated liquid (HP4-HP5) before it is further expanded in the throttle to the evaporating pressure (HP5-HP6). The working fluid evaporates in the heat exchanger (HP6-HP7) by the heat supply from a river and is further heated in the regenerative heat exchanger (HP7-HP1).

Discharging Process

The liquid working fluid is compressed in the pump to a high-pressure level (HE1-HE2). Heat is then transferred to the fluid in the heat exchanger (HE2-HE3), using the two-zone energy storage. In a transcritical process, the fluid is heated with a phase change during temperature decrease, whereas in a subcritical process, the fluid undergoes a phase change at a constant temperature and evaporation also takes place. Then, the working fluid is expanded in the turbine (HE3-HE4), which drives the generator. To close the cycle, the working fluid is condensed in the heat exchanger (HE4-HE1) by releasing the heat to a river and reaches the initial state (HE1).

For the discharging process, a heat engine in transcritical operation mode with the same working fluid (CO_2) as in the charging process was compared with heat engines in subcritical operation mode, using the following working fluids:

- R600a (isobutane), R134a, and R245fa as these fluids are already used in geothermal power plants [16].
- R1233zd(E), as this working fluid is already used in CB laboratory setups [17, 18].
- R1234yf, discussed as replacement fluid for R134a [19].
- R290 (propane), which is used in refrigeration and heat pump systems [20].

2.1. Modeling and Simulation

The modeling and steady-state calculation of the Carnot battery were performed in EBSILON® *Professional* [21]. For this purpose, the components (e.g., the turbine, heat exchanger, and others) are placed on the graphical surface and connected by lines. The line between the components corresponds to electrical, mechanical, or physical lines through which fluids flow. At a point of the physical line, a starting value and the fluid must be defined. With further measuring points, which are to be placed on the corresponding lines, further operating points in the system can be defined. The component 'controller' allows changing an actual value until the setpoint is reached. These controllers are used to determine the mass flow in the subprocesses. For implementing different working fluids, substance databases such as Refprop [22] are available.

The charging process is supplied with 18 MW of electrical power, which is needed to operate the compressor and the two pumps for pumping the river water and the hot water from the two-zone storage. According to [12], the upper pressure and temperature level in HP2 is a maximum of 140 bar and 150 °C, respectively. The maximum storage temperature in ST1 is 115 °C and is based on the already implemented two-zone storage [15]. The heat losses in the two-zone storage tank are neglected in this work. To evaporate the CO_2 in the heat exchanger from HP6-HP7, water is taken from the environment at 10 °C and 1 bar (state: w1), which is reduced by 5 K (state: w3).The temperature in HP6 is determined by specifying a terminal temperature difference or a pinch point in the heat exchanger. This, in turn, results in the evaporation pressure and thus the pressure HP6 and HP7. The same pinch point is specified in all heat exchangers. Pressure losses are also neglected in the process. Isentropic, mechanical, and electrical efficiencies of the components are specified

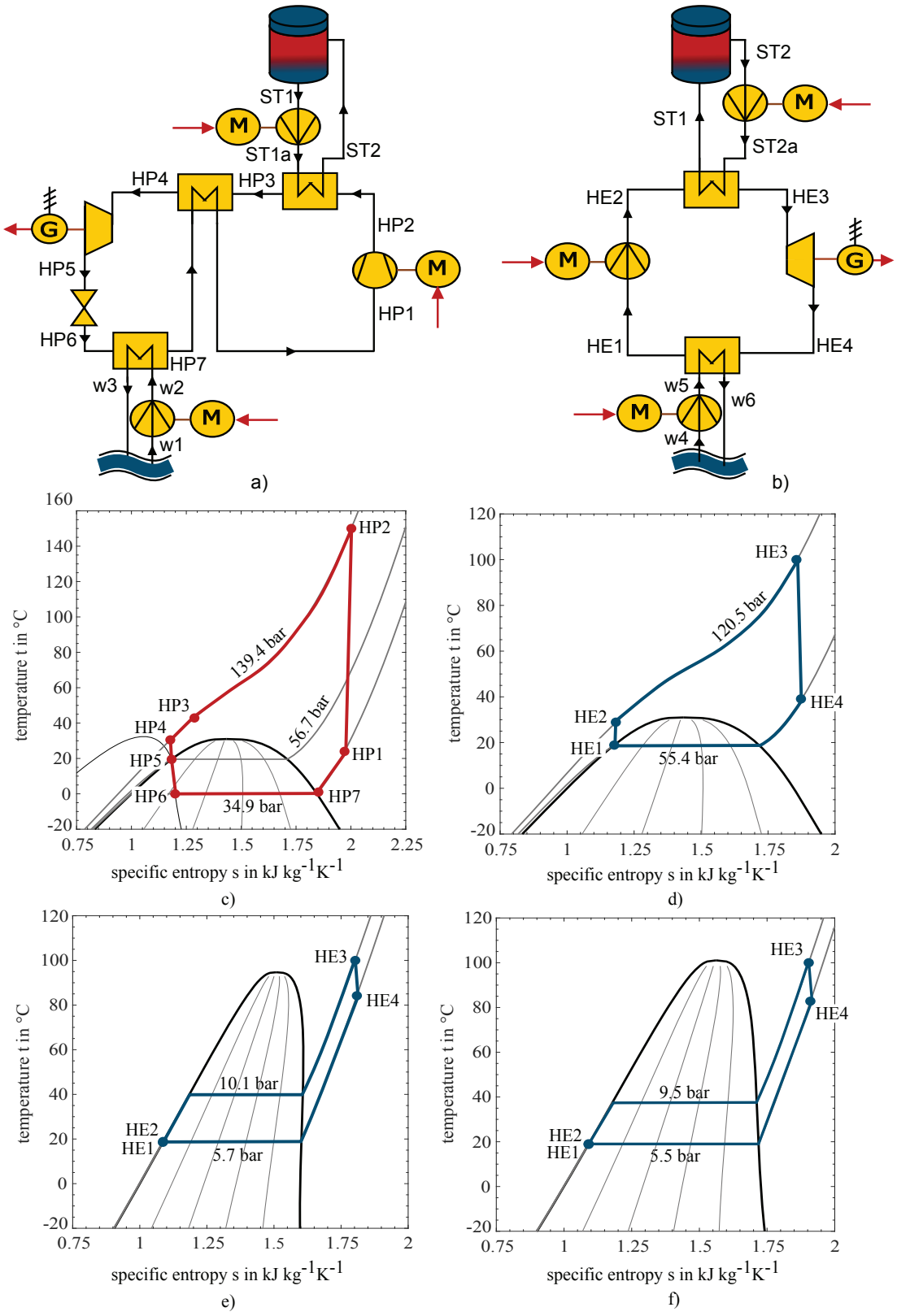

Figure 1: Scheme of the a) charging cycle and b) discharging cycle; t,s diagram of c) charging with CO_2; d) discharging with CO_2; e) discharging with R1234yf and f) discharging with R134a [22].

https://doi.org/10.52202/069564-0192

(see Table A.1). These values are the same for all concepts. As a condition, the lower storage temperature T_{ST1} is defined in such a way that the CO_2 is liquid in state HP4.

2.1.1. Results of the Simulations

Tables 1 and 2 present an overview of the simulation results for the different configurations when two different pinch points are specified. Under a pinch point of 5 K, the transcritical CO_2 discharge process (Configuration 1) achieves the highest round trip efficiency (21.9 %), whereas the other configurations with ORC fluids vary between 9.6 % and 13.7 %. In general, a decrease in pinch point leads to an increase in round trip efficiency. This may be because, the evaporation pressure in the discharge process can be increased and the condensation pressure in the discharge process can be decreased. The overall process of Configuration 1 thus increases in efficiency from 21.92 % to 33.48 %. A greater increase in round trip efficiencies is achieved with Configurations 2-6 (see Figure 2) compared with the pinch point of 5 K. The lower pinch point allows the lower storage temperature T_{ST1} to be increased, which has a positive effect on the heat engine. However, the lower storage temperature is limited upward, otherwise, the state of aggregation before the liquid expander in the heat pump is gaseous. Figure 2 shows the temperature curves of the fluids in the heat exchangers between HP2 and HP3 and between HE2 and HE3, assuming different pinch points. With a reduction of pinch point, the cost of the purchased equipment increases because of the need for a larger heat exchanger area. Considering the LCOE, the financial cost at the expense of efficiency is examined as well. In the following, the working fluids R1233zd(E) and R245fa are not considered for the economic analysis because of the low round trip efficiencies and the low pressure ratios obtained in the discharge process.

Table 1: Results of the simulation with a pinch point of 5 K in the heat exchangers. COP = 3.04, T_{ST1} = 35°C and T_{ST2} = 115°C.

Configuration	1	2	3	4	5	6	7
Discharging process							
Fluid	CO_2	R600a	*R*134*a*	*R*245*fa*	R290	R1234yf	R1233zd(E)
p_{ev} in [bar]	120.5	4.8	9.5	2.2	12.9	10.1	1.8
p_{con} in [bar]	55	2.9	5.5	1.2	8.1	5.7	1.1
η_{HE} in [%]	7.94	3.83	4.28	3.73	4.22	4.48	3.17
η_{rt} **in [%]**	21.92	11.64	13.01	11.35	12.84	13.63	9.65

Table 2: Results of the simulation with a pinch point of 1 K in the heat exchangers.

Configuration	1	2	3	4	5	6	7
Charging process							
Fluid	CO_2	CO_2	CO_2	CO_2	CO_2	CO_2	CO_2
COP in [-]	3.57	3.24	3.2	3.19	3.20	3.21	3.20
TES							
T_{ST1} in [°C]	30.9	41.1	42.4	42.3	42.4	41.8	42.4
Discharging process							
Fluid	CO_2	R600a	*R*134*a*	*R*245*fa*	R290	R1234yf	R1233zd(E)
p_{ev} in [bar]	140	7.9	17.3	4.2	21.8	18.4	3.3
p_{con} in [bar]	51	2.6	5.0	1.0	7.7	5.1	1
η_{HE} in [%]	9.39	8.45	9.40	8.69	9.41	9.47	7.83
η_{rt} **in [%]**	33.48	27.38	30.03	27.77	30.07	30.44	25.03

3. Economic Analysis

This subchapter describes the methods used for calculating the purchased equipment costs (PECs) as well as the levelized cost of electricity (LCOE).

3.1. Equipment Cost

In addition to its efficiency, the cost of a CB is also important. For a first estimation of component costs, the Turton method [23] was used. With this method, the PECs are calculated on the basis of cost functions, which result from predefined factors and characteristic size parameters, such as the power or heat exchanger area.The estimation of the PEC of the generators' was based on the six-tenths rule [24]. The reference values were obtained from the cost of the generator by Balli et al. [25]. The PEC of the throttle was negligible compared to the other components. A detailed description for estimating PEC is available at [26]. For calculating the PEC

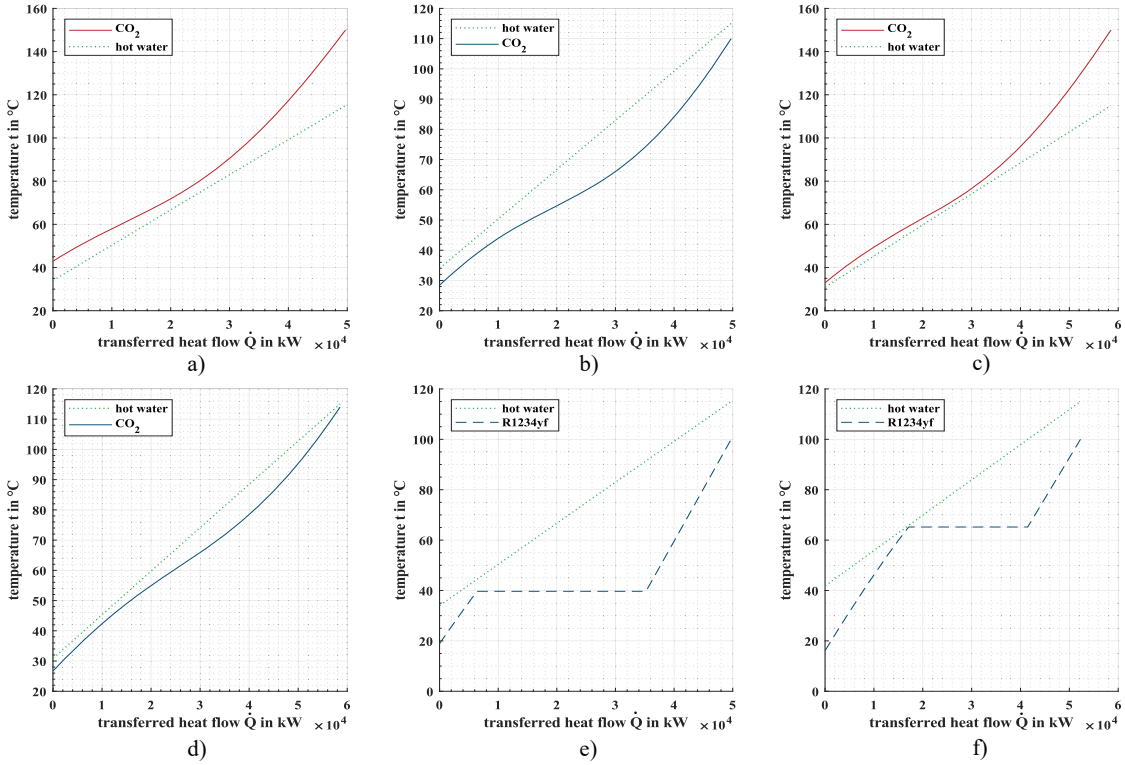

Figure 2: t,Q diagram of a) Configuration 1 in the heat exchanger (HP2-HP3) with pinch point= 5 K; b) Configuration 1 in the heat exchanger (HE2-HE3) with pinch point= 5 K; c) Configuration 1 in the heat exchanger (HP2-HP3) with pinch point= 1 K; d) Configuration 1 in the heat exchanger (HE2-HE3) with pinch point= 5 K; e) Configuration 6 in the heat exchanger (HE2-HE3) with pinch point= 5 K; f) Configuration 6 in the heat exchanger (HE2-HE3) with pinch point= 1 K for illustration of the curve between the fluids.

of the two-zone storage tank, an average value of 550 €/m^3 [15] was applied. The PECs are based on specific reference years. Hence, it is necessary to update costs by considering the price development, inflation, and other factors, with the aid of the cost index Chemical Engineering Plant Cost Index (CEPCI). For the selected reference year (2021), the CEPCI was 708 [27]. The official exchange rate of the European Commission [28] was applied for converting other currencies into euros.

3.2. Levelized Cost of Electricity

For comparing the CB configurations, LCOE was calculated according to [29]. The LCOE is composed of the economic expenditure of the system during its lifetime and the total amount of electricity generated. Taking into account the purchase cost of the supplied electrical energy $c_{\mathrm{el,in}}$, the LCOE can be calculated according to the following equation:

$$LCOE = \frac{I + \sum_{t=1}^{n} \frac{A_t}{(1+i)^t}}{\sum_{t=1}^{n} \frac{En_{t,\mathrm{el}}}{(1+i)^t}} + \frac{c_{\mathrm{el}}}{\eta_{\mathrm{rt}}}. \tag{1}$$

The time period is set to n = 25 years. The aim is to operate the CB 365 days a year with a uniform charging and dicharging time of $\Delta\tau$ = 4 h. This results in the annually produced amount of electricity $En_{t,\mathrm{el}}$ with $En_{t,\mathrm{el}} = 365 \cdot \Delta\tau \cdot P_{\mathrm{out}}$. The investment costs I include not only the PECs, but also take into account other costs (e.g., for pipes, measuring devices and installation) [30]. To determine the investment costs I, the total PECs are multiplied by the Lang factor ($F_{\mathrm{Lang}} = 4.74$) [30]. The annual operation and maintenance costs A_t are determined using a constant factor $F_{\mathrm{op}} = 0.015$. This factor (F_{op}) is multiplied by the total investment costs.The purchase cost $c_{\mathrm{el,in}}$ of the supplied electrical power during charging is determined using the day-ahead market for Germany and Austria of the European Energy Exchange. Application of the approach of Dietrich [31] to the reference year 2021 results in a purchase cost of $c_{\mathrm{el,in}}$ = 6.64 €cents/(kWh)$^{-1}$ [32]. The debt interest rate i is estimated from the program 'Renewable Energies Standard' [33] of the credit bank KfW. This program is

https://doi.org/10.52202/069564-0192

finances renewable energy systems such as battery storage and power-to-X systems and enables debt capital financing of 100 %. A debt interest rate of i = 3.49 % [34] was selected for the program at a maximum fixed interest period of 20 years. Because the period of time is 25 years in this study, we assumed that the interest rate remains fixed and does not change over the additional 5 years. No adjustments for inflation were made.

3.3. Results of the Economic Analysis

Table 3 gives an overview of the total PEC and LCOE of the different configurations for a uniform charging and discharging time of 4 h at a pinch point of 5 K in all heat exchangers. The total PEC of the subcritical processes of Configurations 1-3,5,6 averages $12.209 \cdot 10^6$ €. Configuration 1, based on the CO_2 HE, has PECs about 3 million euro higher than others. Despite, Configuration 1 has the lowest LCOE (123 €cents $(kWh)^{-1}$). The other configurations are in the range of 183-214 €cents $(kWh)^{-1}$ because of their poor round trip efficiency. With the decrease in pinch point, component costs for Configuration 1 increased by almost 57 %, whereas the other configurations became on average 20 % more expensive (see Table 4). A higher LCOE for Configuration 1 was obtained. This is mainly due to the increased costs for the heat exchangers, resulting from the reduced temperature differences within them in the heat engine, from the hot TES to the discharging process. For the other configurations, a reduction in pinch point had a positive effect on LCOE, which was reduced by 50 % on average. Tables 5 and 6 show that the LCOEs were further reduced with a uniform charging and discharging time of 5 and 6 h, respectively. The two-zone storage system should be larger, but this additional cost does not affect the total PEC or the LCOE as much. In addition, Fig. 3 compares the shares of the PECs of the different components for Configuration 1 (CO_2) and for Configuration 6 (R1234yf) with different pinch points. The subprocesses of charging, storage, and discharging are presented in different colors. For all variants, the compressor (including the motor) is the most cost-intensive component, but with a lower pinch point, the cost proportion of the heat exchangers increases. The distributions of the PECs of the other configurations are similar to Configuration 6.

Table 3: PEC and LCOE with a pinch point of 5 K in heat exchangers during uniform charging and discharging for 4 h.

Configuration	1	2	3	5	6
PEC [10^6 €]	15.387	12.152	12.213	12.236	12.233
LCOE [€cents $(kWh)^{-1}$]	123	214	192	195	183

Table 4: PEC and LCOE with a pinch point of 1 K in heat exchangers during uniform charging and discharging for 4 h.

Configuration	1	2	3	5	6
PEC [10^6 €]	24.118	14.670	14.683	14.712	14.751
LCOE [€cents $(kWh)^{-1}$]	128	105	96	96	95

Table 5: LCOE with a pinch point of 5 K in heat exchangers during uniform charging and discharging for 5 h with $c_{el,in}$ = 6.8 € cents $(kWh)^{-1}$

Configuration	1	2	3	5	6
PEC [10^6 €]	15.685	12.449	12.512	12.535	12.532
LCOE €cents $(kWh)^{-1}$	106	187	168	170	160

Table 6: LCOE with a pinch point of 5 K in heat exchangers during uniform charging and discharging for 6 h with $c_{el,in}$ = 7 € cents $(kWh)^{-1}$

Configuration	1	2	3	5	6
PEC [10^6 €]	15.984	12.747	12.810	12.833	12.830
LCOE [€cents $(kWh)^{-1}$]	95	169	152	154	145

3.4. Sensitivity Analysis of the LCOE

A sensitivity analysis was performed to identify the parameters with the most substantial effects on the LCOE. Table 7 lists the parameters and the corresponding results of the sensitivity analysis. The results of one configuration are shown in this work, because they are comparable to those of the other configurations. Only the absolute values differed among configurations. The fluctuation of the purchase costs exerted the greatest influence on the LCOE. The lower and upper limits of the purchase costs corresponded to 2020 and 2022, respectively. With a relative deviation of around 18.7 %, investment costs also have a major influence on the LCOE. Fluctuations between 6 and 10 percent occur with different period of time and debt interest rate. Due

to the large uncertainties in LCOE, these configurations are not suitable to evaluate economic viability. In this work, LCOE is applied to compare the different configurations.

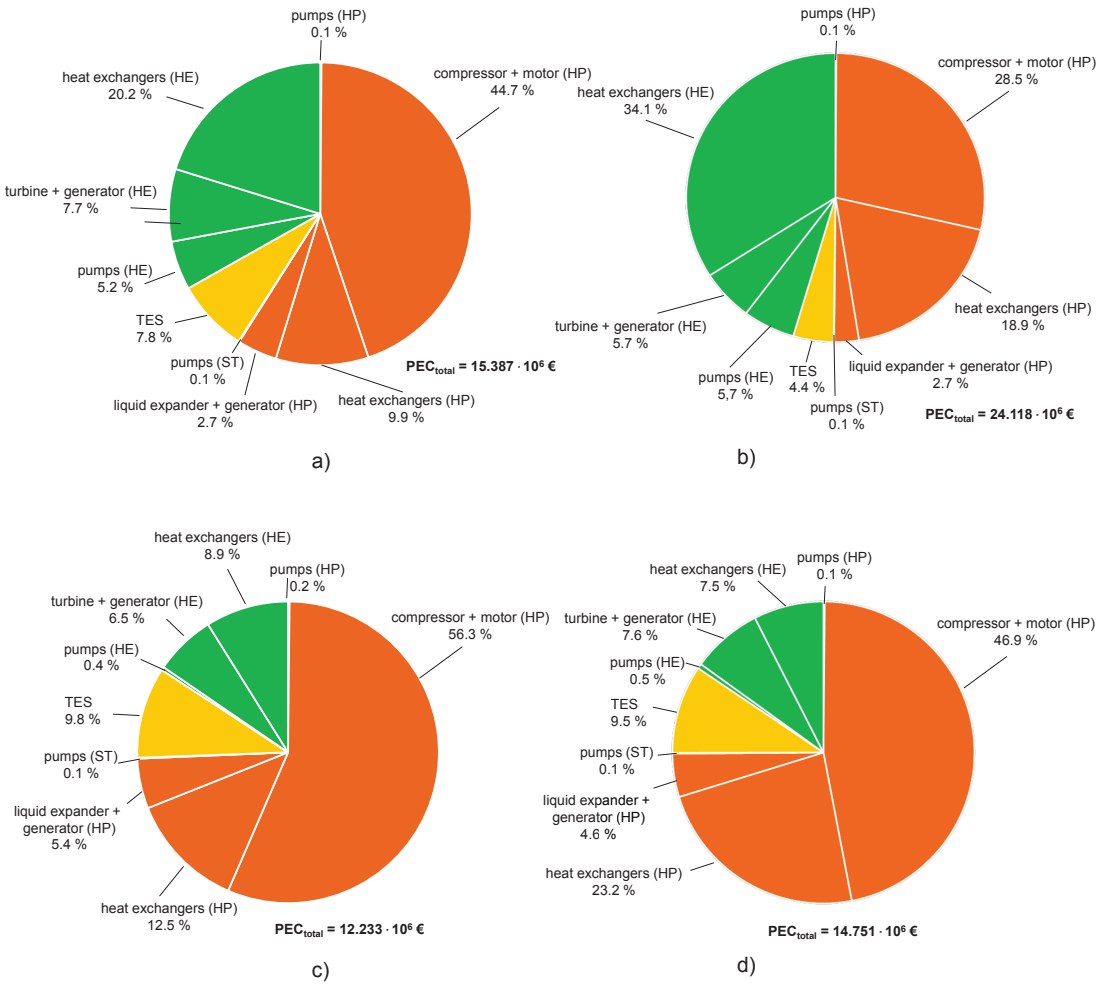

Figure 3: PEC distribution for configuration 1 a) with a pinch point of 5 K, b) with a pinch point of 1 K and for configuration 6 a) with a pinch point of 5 K and b) with a pinch point of 1 K.

Table 7: Sensitivity analysis of the LCOE for configuration 1 with a pinch point of 5 K

Parameter	**Value**	**Variation of LCOE**
Investment costs I	0.7 · $I_{\text{base case}}$	-18.68 %
(base case: 72.935 · 10^6 €)	1.3 · $I_{\text{base case}}$	+18.68 %
Factor for operational costs F_{op}	1 %	-5.14 %
(base case: 1.5 %)	2 %	+5.14 %
Period of time n	20 years	+9.95 %
(base case: 25 years)	30 years	-6.48 %
Debt interest rate i	2.39 % [34]	-7.20 %
(base case: 3.49%)	4.69 % [34]	+8.38 %
Purchase cost of electricity $c_{\text{el,in}}$	1.82 €cents (kWh)$^{-1}$	-16.21 %
(base case: 6.64 €cents (kWh)$^{-1}$)	16.31 €cents (kWh)$^{-1}$	+32.54 %

4. Technology Readiness Level

The technology readiness level (TRL) scale of the European Commission [35] is a method used to assess the maturity and readiness of a technology or concept. The TRL scale ranges from 1 to 9, with 1 being the

https://doi.org/10.52202/069564-0192

Table 8: TRL scale [35]

Phase	TRL level	Condition
Research	1	Basic principles observed
	2	Technology concept formulated
	3	Experimental proof of concept
Development	4	Technology validated in lab
	5	Technology validated in relevant environment
	6	Technology pilot demonstrated in relevant environment
Deployment	7	System prototype demonstration in operational environment
	8	System complete and qualified
	9	Actual system proven in operational environment

lowest level of technological maturity and 9 being the highest. In the following section, the TRL is applied to the subprocesses.

4.1. Evaluation of the Subprocesses

CO_2 heat pump
CO_2 heat pumps using positive displacement machines and throttle for expanding CO_2 are already offered on the market. However, these are limited in their capacities [14]. A configuration similar to the concept in this study was developed and successfully implemented in the form of a test rig by MAN Energy Solutions [12, 13]. The necessary components are also offered by this company. Instead of a displacement machine a barrel compressor is used, enabling a higher capacity. As a result, the subprocess is classified as TRL6. Since there is not evidence yet of a prototype in a relevant operational environment, a TRL of 7 is not achieved.

Two-zone storage
This storage system is assigned a TRL of 8 because it is already being used in various facilities [15], but is not yet in mass production.

CO_2 heat engine
The CO_2 discharging process has been studied experimentally [36]. Therefore, a TRL of at least 3 is achieved. One manufacturer offers a commercial system [37] based on a supercritical process and with high temperature heat supply. In our study, a lower heat supply temperature of 115 °C is used. Consequently, the subprocess is assessed as TRL = 5, and still needs further testing and development under operational conditions to achieve a TRL of 6.

ORC with R600a
In Grünwald, Germany [16], an ORC process with isobutane as the working fluid is already used to generate electricity. An electrical output of 4.3 MW is achieved at a geothermal spring inlet temperature of 135 °C,. Consequently, the subprocess achieves a TRL of 8.

ORC with R134a
A geothermal power plant using the working fluid R134a is in operation. The power plant is able to generate 5.5 MW of electrical power using a geothermal spring with an inlet temperature of 118 °C [16]. Therefore, the HE is assigned a TRL of 8.

ORC with R290
Propane is widely used as a working fluid in refrigeration systems [20]. So far, only one research group [38] is known to use propane in their transcritical process for geothermal power generation. Hence, the subprocess results in a TRL of 5.

ORC with R1234yf
R1234yf was developed as a replacement for R134a. ORC with this working fluid has been investigated and verified through numerical simulations, achieving a TRL of 3. However, a prototype or experimental investigation has not yet been developed or conducted, which is necessary to achieve a TRL of 4 [19].

4.2. Evaluation of the Overall Process

The TRL of the overall processes is determined by the lowest TRL resulting from the subprocesses. Configurations 2 with R600a and 3 with R134a reach the highest TRL level with 6. The lowest TRL level is reached by configuration 6 with R1234yf.

5. Discussion

Under the assumption of a pinch point of 5 K, the investigated configurations achieved round trip efficiencies between 9 % and 22 % and LCOEs between 123 and 214 €cents $(kWh)^{-1}$, with Configuration 1 using CO_2 in

the heat engine process achieving the best results. Reducing the pinch point demonstrated that configurations using subcritical processes result in better round trip efficiencies and substantially lower LCOEs. Compared to Configuration 1 with CO_2 in the discharge process, increasing efficiency by 11.5 % results in a higher LCOE because in the greater heat transfer surface area between the hot water and CO_2 during the discharge. This results in high component costs. Configurations 2 and 3 with R600a and R134a, respectively, achieved the highest overall TRL and therefore enable prompt implementation. The ORC fluid R134 achieved better results compared to isobutane. However, because of its high global warming potential (GWP), this fluid may be excluded from ORC processes in the future by the European Union.

Although Configuration 1 with a pinch point of 5 K showed the highest round trip efficiency, the lowest LCOE, and an overall TRL of 5, this combination with the environment as a heat reservoir is unsuitable because if the ambient temperature increases, the evaporating pressure and temperature in the heat engine approach the critical point of CO_2, leading to technical problems. One possibility is the combination of an ice storage with an intermediate circuit. However, in this case, a heat exchanger must be integrated into the process to dissipate the heat generated by irreversibilities from the system to the environment. Nevertheless, indirect ice storage adds further costs and irreversibility.

CBs based on transcritical CO_2 cycles showed a substantially higher round trip efficiency in some studies [4, 7–9, 11]. The reason for this is primarily due to the utilization of different CBs. First, the CBs use a second storage tank at a low temperature, integrated directly into the subprocesses, either with ice slurry storage [9] or ice storage [7]. Because of the high pressure of the working fluid (CO_2), ice storage is not feasible [13]. Ice slurry storage tanks are uncommon [39], resulting in a lower TRL level. Higher round trip efficiencies also result for pressurized tanks with water at high storage temperatures, as shown in previous publication [4]. Moreover, multiple high-temperature storage tanks are employed to improve the temperature glide between CO_2 and the storage medium (water). This necessitates the use of multiple heat exchangers, which substantially increase the complexity of the system.

Furthermore, unlike the approach taken in this study, many publications do not account for losses in the motors and generators, and rely solely on machine for the expansion process during charging, which could make the system unfeasible from a technical point of view.

Another improvement in round trip efficiency is achieved through supercritical discharge processes and ORC fluids as working fluids [11]. However, this requires higher storage temperatures and the use of alternative storage media in case the storage medium exceeds 160 °C. Furthermore, an appropriate compressor that can achieve high temperatures is needed for the charging process. Consequently, a low TRL is expected.

Under simplified assumptions, such as the absence of storage heat and pressure losses, the actual forward and return efficiencies of the system are expected to be lower than those predicted by the configurations.

6. Conclusion and Outlook

In this study, CBs based on a transcritical CO_2 charging process with an electrical power input of 18 MW were numerically modeled and simulated stationarily, using the Ebsilon software. A two-zone storage tank with water as a storage medium at a maximum temperature of 115 °C was used. For the discharge, a transcritical CO_2 process and subcritical processes with different organic working fluids were investigated and compared to each other on the basis of round trip efficiency, LCOE, and TRL. With a pinch point of 5 K, Configuration 1 (transcritical CO_2 HE) resulted in the highest round trip efficiency and the lowest LCOE. Despite an overall TRL of 5, this configuration is unsuitable for implementation because the operating points of the evaporator in the HE approach the critical point as the ambient temperature increases, which could lead to technical problems. The other configurations resulted in very low round trip efficiencies, leading to a high LCOE. By reducing the pinch point in the heat exchangers, the efficiencies can be increased, which has a positive effect on the LCOE. Among the subcritical processes, the working fluid R1234yf (Configuration 6) could be an alternative. However, this variant was classified with the lowest TRL level. Similar round trip efficiencies and LCOE at a higher TRL level were achieved with the ORC fluid R134a (Configuration 3). However, the refrigerant R134a has a high global warming potential and is already banned in the automotive sector [40]. The same TRL level was achieved with R600a (Configuration 2), which has the highest LCOE due to its poorer round trip efficiency. The economic values were estimated under considerable uncertainties, as the sensitivity analysis on LCOE showed. Detailed information on component costs and a full financing calculation are required for an economic evaluation of the configurations, as well as the specifications of an accurate plant design, such as the isentropic efficiency of the turbine, compressor, and pumps. With a uniform charging and discharging time of 4 h, the LCOEs are very high, but can be reduced if the charging and discharging duration increases. Because Configuration 1 is excluded as a possible option in this study, replacing the environment as a storage unit with ice could be considered in further investigations to obtain an overview of the possible round trip efficiency, LCOE, and TRL compared to the configurations studied here.

https://doi.org/10.52202/069564-0192

Appendix A

Table A.1: Component parameters used in Ebsilon

Parameter	Symbol	Value	Unit
Isentropic efficiency compressor	$\eta_{is,compressor}$	85	%
Isentropic efficiency liquid expander	$\eta_{is,expander}$	85	%
Isentropic efficiency pumps	$\eta_{is,pump}$	80	%
Isentropic efficiency turbine	$\eta_{is,turbine}$	85	%
Mechanical efficiency compressor	$\eta_{mech,compressor}$	99	%
Mechanical efficiency liquid expander	$\eta_{mech,expander}$	99	%
Mechanical efficiency pumps	$\eta_{mech,pump}$	99	%
Mechanical efficiency turbine	$\eta_{mech,turbine}$	99	%
Mechanical efficiency motor	$\eta_{mech,motor}$	99	%
Electrical efficiency motor	$\eta_{el,motor}$	95	%
Electrical efficiency generator	$\eta_{el,generator}$	98	%

References

[1] European Power Exchange, *EPEX SPOT SE.* `https://www.epexspot.com` [accessed 12.03.2023]

[2] Liang, T., Vecchi, A., Knobloch, K., Sciacovelli, A., Engelbrecht, K., Li, Y., Ding, Y., *Key components for Carnot Battery: Technology review, technical barriers and selection criteria.* Renewable and Sustainable Energy Reviews 2022;163:112478.

[3] Zhao, Y., Song, J., Liu, M., Zhao, Y., Olympios, A. V., Sapin, P., Yan, J., Markides, C. N., *Thermo-economic assessments of pumped-thermal electricity storage systems employing sensible heat storage materials.* Renewable Energy 2022;186:431-456.

[4] Morandin, M., Marchal, F., Mercangöz, M., Buchter, F., *Conceptual design of a thermo-electrical energy storage system based on heat integration of thermodynamic cycles Part A: Methodology and base case.* Energy 2012;45(1):375-385.

[5] Morandin, M., Marchal, F., Mercangöz, M., Buchter, F., *Conceptual design of a thermo-electrical energy storage system based on heat integration of thermodynamic cycles Part B: Alternative system configurations.* Energy 2012;45(1):386-396.

[6] Morandin, M., Mercangöz, M., Hemrle, J., Marchal, F., Favrat, D., *Thermoeconomic design optimization of a thermo-electric energy storage system based on transcritical CO_2 cycles.* Energy 2013;58:571-587.

[7] Steinmann, W.D., Jockenhöfer, H., Bauer, D., *Thermodynamic Analysis of HighTemperature Carnot Battery Concepts.* Energy Technol. 2020;8(3):1900895.

[8] Kim, Y.-M., Shin, D.G., Lee, S.Y., Favrat, D., *Isothermal transcritical CO_2 cycles with TES (thermal energy storage) for electricity storage.* Energy 2012;49:484-501.

[9] Mercangöz, M., Hemrle, J., Kaufmann, L., ZGraggen, A., Ohler, C., *Electrothermal energy storage with transcritical CO_2 cycles.* Energy 2012;45(1):407-415.

[10] Baik, Y.J., Heo, J., Koo, J., Kim, M., *The effect of storage temperature on the performance of a thermo-electric energy storage using a transcritical CO_2 cycle.* Energy 2014;75:204-215.

[11] Koen, A., Farres Antunez, P., White, A., *A study of working fluids for transcritical pumped thermal energy storage cycles* In: 2019 Offshore Energy and Storage Summit (OSES), 2019 Jul 10-12, Brest, France. p.1-7.

[12] Hirsch T. *MAN Wärmepumpen-Wie wir die klimaneutrale Zukunft der Stadt Esbjerg gestalten.* 27. Dresdner Fernwärme-Kolloquium, 2022.

[13] Decorvet R.C., Jacquemoud E., *Industrial heat pumps - MAN Energy Solutions.* Research report, 2021. `https://www.man-es.com/campaigns/download-request` [accessed 03.02.2023]

[14] Cordin Arpagaus, Frdric Bless, Michael Uhlmann, Jürg Schiffmann, Stefan S. Bertsch, *High temperature heat pumps: Market overview, state of the art, research status, refrigerants, and application potentials.* Energy 2018;152:985-1010.

[15] Maximini M., *Flexibilisierung der Strom- und Wärmeerzeugung durch Wärmespeicher.* Available at: `https://enerko.de/wp-content/uploads/2019/11/191120-Flexibilisierung-der-Strom-und-Waermeerzeugung-durch-Waermespeicher-.pdf` [accessed 08.02.2023]

[16] Heberle F., Brüggemann D., Weiß A.P., Grundemann L., *Geothermische Kraftwerke in Deutschland: Individuelle Lösungen durch die geeignete Wahl des Arbeitsmediums.* In: BWK: Das Energie-Fachmagazin 2017;69(6):51-54.

[17] Dumont, O., Charalampidis, A., Lemort, V., *Experimental Investigation Of A Thermally Integrated Carnot Battery Using A Reversible Heat Pump/Organic Rankine Cycle.* In: Proceedings of the International Refrigeration and Air Conditioning Conference, 2021.

[18] Eppinger, B., Steger, D., Regensburger, C., Karl, J., Schlücker, E., Will, S., *Carnot battery: Simulation and design of a reversible heat pump-organic Rankine cycle pilot plant.* Applied Energy 2021;288:116650.

[19] Garca-Pabn J.J., Mndez-Mndez D., Belman-Flores J.M., Barroso-Maldonado J.M., Khosravi A. *A Review of Recent Research on the Use of R1234yf as an Environmentally Friendly Fluid in the Organic Rankine Cycle.* Sustainability. 2021; 13(11):5864.

[20] Redouane Ghoubali, Paul Byrne, Frdric Bazantay, *Refrigerant charge optimisation for propane heat pump water heaters*International Journal of Refrigeration 2017;76:230-244.

[21] Iqony Solutions GmbH, *EBSILON® Professional, Process Simulation Software*. Available at: `https://systemtechnologies.iqony.energy/de` [accessed 03.02.2023]

[22] Lemmon, E.W., Bell, I.H., Huber, M.L., McLinden, M.O. *NIST Standard Reference Database 23: Reference Fluid Thermodynamic and Transport Properties-REFPROP.* Version 9.1, National Institute of Standards and Technology, 2013.

[23] Turton R., Bailie R. C., Whiting W.B., Shaeiwitz J.A., Bhattacharyya D., *Analysis, synthesis, and design of chemical processes.* Pearson, Upper Saddle River, 4th edition, 2013.

[24] A. Bejan, G. Tsatsaronis, M. Moran, *Thermal Design and Optimization.* Wiley-Interscience publication, Wiley, 1996.

[25] Balli O., Aras H., Hepbasli A., *Exergoeconomic analysis of a combined heat and power (CHP) system*. International Journal of Energy Research 2008;32(4):273-289.

[26] Koksharov J., Teles de Oliveira H., Dammel F., Stephan P., *Evaluation of different pumped thermal energy storage systems*. In: Amano, Y., Sciubba, E., Elmegaard, B. (Editors). ECOS 2021: Proceedings of the 34th International Conference on Efficiency, Cost, Optimization, Simulation and Environmental Impact of Energy Systems; 2021 Jun 27 - Jul 2; Taormina, Italy. p. 679-690.

[27] Towering Skills, *Cost Indices,* Available at: `https://www.toweringskills.com/financial-analysis/cost-indices/` [accessed 23.02.2023].

[28] European Commission, *Exchange rate.* Available at: `https://www.ecb.europa.eu/stats/policy_and_exchange_rates/euro_reference_exchange_rates/html/eurofxref-graph-usd.de.html` [accessed 08.02.2023]

[29] Kost C.,Shammugam S.,Fluri V., Peper D., Memar A.D., Schlegl T., *Stromgestehungskosten Erneuerbare Energien*. Study, Jun 2021.

[30] Towler G.P., Sinnott R.K., *Chemical Engineering Design: Principles, Practice, and Economics of Plant and Process Design.* Butterworth-Heinemann, Boston, MA, 2nd edition, 2013.

[31] Dietrich A., *Assessment of Pumped Heat Electricity Storage Systems through Exergoeconomic Analyses [dissertation]* Darmstadt, Germany: TU Darmstadt; 2017.

[32] entsoe, *Transparency Platform.* Available at: `https://transparency.entsoe.eu` [accessed 23.02.2023].

[33] KfW, *KfW-Programm Erneuerbare Energien 'Standard'.* Available at: `https://www.kfw.de/inlandsfoerderung/Unternehmen/Wohnwirtschaft/F\unhbox\voidb@x\bgroup\accent127o\penalty\@M\hskip\z@skip\egrouprderprodukte/Erneuerbare-Energien-Standard-(270)` [accessed 23.02.2023].

[34] KfW, *Konditionenübersicht für Endkreditnehmer.* `https://www.kfw-formularsammlung.de/KonditionenanzeigerINet/KonditionenAnzeiger` [accessed 01.06.2021].

[35] De Rose A., Buna M., Strazza C., Olivieri N., Stevens T., Peeters L., Tawil-Jamault D., *Technology Readiness Level: Guidance Principles for Renewable Energy technologies.* Report, 2017.

[36] Lecompte S, Ntavou E, Tchanche B, Kosmadakis G, Pillai A, Manolakos D, De Paepe M. *Review of Experimental Research on Supercritical and Transcritical Thermodynamic Cycles Designed for Heat Recovery Application.* Applied Sciences. 2019;9(12):2571

[37] Echogen Power Systems, *EPS100 Heat Recovery Solution.* Available at: `https://www.echogen.com/_CE/pagecontent/Documents/EPS100_brochure_2017.pdf` [accessed 02.03.2023]

[38] Gardella L., Wiemer H.-J. *First experimental results of a supercritical Organic Rankine cycle using propane as working fluid.* Annual Report 2020 of the Institute for Thermal Energy Technology and Safety. Editor: W. Tromm, KIT Scientific Publishing, 2022.p.59-65.

[39] Dincer I., Erdemir D., *Heat Storage Systems for Buildings; Chapter 2 - Heat Storage Methods.* Elsevier, 2021.p. 3790.

[40] Macchi E., Astolfi M., *Organic Rankine Cycle (ORC) Power Systems, Technologies and Applications.* Woodhead Publishing, 2017.

 https://doi.org/10.52202/069564-0192